Phase front design with metallic pillar arrays

Lieven Verslegers, Peter B. Catrysse, Zongfu Yu, Wonseok Shin, Zhichao Ruan, and Shanhui Fan*

E. L. Ginzton Laboratory and Department of Electrical Engineering,
Stanford University, Stanford, California 94305, USA
*Corresponding author: shanhui@stanford.edu

We demonstrate numerically, using a three-dimensional finite-difference frequency-domain method, the ability to design a phase front using an array of metallic pillars. We show that in such structures, the local phase delay upon transmission can be tuned by local geometry. We apply this knowledge to demonstrate a metallic microlens. The presented design principles apply to a wider range of wavelength-size integrated photonic components. © 2010 Optical Society of America

OCIS codes: 310.6628, 250.5403, 230.0230, 310.6805.

A variety of compact photonic devices based on the manipulation of light by nanostructured metals has been suggested and demonstrated recently [1–3]. Slit arrays in an optically thick metallic film, for example, were proposed as a means to achieve phase front control for the focusing and redirecting of light [4–10]. The use of nanostructured metal films to control the phase front provides several advantages over conventional shaped dielectrics, including a larger index contrast, greater design freedom, and a planar geometry that facilitates integration while being compatible with existing manufacturing techniques [8]. A limitation of phase control with slit arrays, however, is that slits provide control in one dimension only. Moreover, these structures are essentially polarizing devices.

Three-dimensional variations on the slit array structure have been suggested to address such limitations, but the published designs also forego some of the advantages of slit arrays. Arrays of square holes with different sizes in a metallic film have been shown to act as lenses with focusing capabilities in two dimensions [11]. Such structures, however, rely on the presence of a propagating mode in each hole, which dictates the size of the hole to be at least half a wavelength, and, hence, prevents scaling of the entire device to sizes on the order of a wavelength. In a different approach, a microzone plate, based on the principle of diffraction, was shown to focus an incident plane wave into a subwavelength spot [12]. This microzone plate, however, is strongly polarization dependent, fairly large, and has a circular shape that is undesirable in the context of periodic arrays of such elements on a square lattice, e.g., square lenses are preferable from a light collection and real-estate perspective.

In this Letter, we numerically demonstrate the ability to perform phase front design in two dimensions by varying the local geometry in metallic nanoscale pillar arrays. Our approach maintains the advantages of nanoscale slit arrays while overcoming its limitations. The proposed structure is planar, can be made polarization independent, and is well suited to miniaturization because its building blocks can be made much smaller than a wavelength. We demonstrate the design freedom that is offered by metallic pillar arrays through the simulation of a wavelength-size metallic microlens. The design principles are more general though and could be applied to a larger range of compact photonic devices for the benefit of controlling the incoupling and outcoupling of light.

Figure 1 shows an example structure that is based on a two-dimensional array of square gold pillars with varying base size depending on location within the array. The pillars are 400 nm tall and have base sizes ranging from 25 to 75 nm. They are centered in 100 nm by 100 nm unit cells that are organized on an 11 by 11 grid. The structure operates on light incident along the z direction. The calculations and simulations are performed for a y-polarized plane wave with a wavelength of 632.8 nm. The permittivity of gold at this wavelength is $\varepsilon_m = -10.78 + 0.79i$ [13]. For simulation purposes, we opt for this structure to repeat itself in the x and y directions. The simulation results then correspond to the case of a periodic array of microlenses. Microlens arrays are very common in practical applications, where microlenses are often placed on top of a photodetector array to improve the individual detector efficiency [9]. The array geometry also eliminates any effects that might occur owing to the small aperture size of individual microlenses [8,14].

The purpose of the metallic pillar array is to create a position-dependent phase delay as light propagates
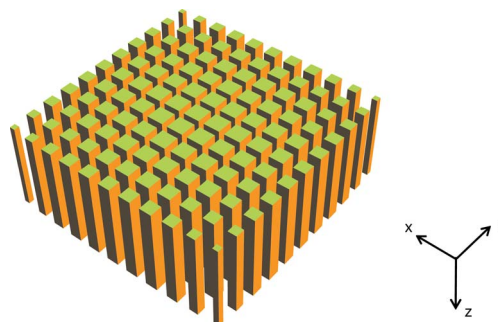
Fig. 1. (Color online) Metallic nanoscale pillar array for two-dimensional phase front design. The entire structure is on the order of the wavelength size and consists of an array of 11 by 11 unit cells with 400 nm tall gold pillars of variable base width (between 25 and 75 nm) in unit cells of 100 nm by 100 nm.

through the structure. To calculate the phase delay associated with light propagation through a local region consisting of a single nanoscale pillar, we calculate the complex propagation constant $\beta = \beta_R + i\beta_I$ of the symmetric eigenmode of a periodic array of nanoscale pillars of infinite length using a full-vector finite-difference frequency-domain (FDFD) mode solver [15]. The symmetric eigenmode is relevant because this is the mode that a plane wave incident along the normal direction couples to. The phase delay through the local region is then estimated as $\beta_R d$, where the distance d corresponds to the thickness of the nanopatterned metallic film, i.e., the height of the pillars. The complex propagation constant β depends strongly on the cross-sectional size of the pillar [Fig. 2(a)]. The real part of the effective index is defined as $n_R = \beta_R / k_0$, with k_0 the free space propagation constant, and ranges from one for vacuum to more than three for $s = 0.9a = 90$ nm, where $a = 100$ nm is the size of the unit cell. In all cases considered, $n_R \gg n_I (= \beta_I / k_0)$, and material losses do not obscure the phase delay effect over the thickness of the structure.

Figure 2(b) shows a vector plot of the electric field for the symmetric eigenmode in the array that corresponds to a pillar with $s = 65$ nm. The electric field concentrates in the gap between the metal pillars. For a y-polarized (x-polarized) plane wave, the corresponding eigenmodes have their electric field concentrate at the top/bottom (left/right) sides of the unit cell. These two modes are degenerate, having the same effective index.

Based on the properties of the eigenmodes of an individual element as outlined above, we now design a wavelength-size microlens based on an array of such elements. To achieve lensing, for an incident plane-wave front, the metallic pillar array needs to generate an outgoing phase front that is curved. The required phase delay ideally has the following form:

$$\phi(x,y) = \frac{2\pi f}{\lambda} - \frac{2\pi \sqrt{f^2 + x^2 + y^2}}{\lambda}, \qquad (1)$$

given as a function of position x and y, as measured from the center of the lens, where λ is the wavelength, and f is the geometrical focal length. This analytical phase delay is shown, up to an arbitrary
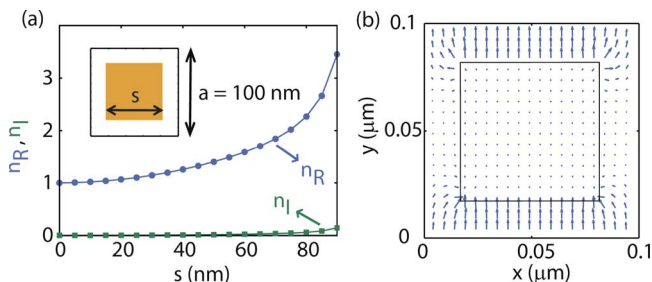
constant, in Fig. 3(a) for $f = 0.5$ μm. It can be approximated by picking the correct pillar size, which results in a local phase delay of $\beta_R d$, for each unit cell. This approximate phase delay, corresponding to the structure from Fig. 1, is shown in Fig. 3(b).

The microlens design is validated with full three-dimensional FDFD simulations of the entire structure [16,17]. This method allows us to model materials using the measured, tabulated permittivity for every wavelength, thus directly taking into account both exact material dispersion as well as loss. For this simulation, we set the grid size to 5 nm in the transverse x and y directions and 20 nm in the longitudinal z direction, resulting in a manageable simulation domain size. This allows us to find the phase past the exit surface [Fig. 3(c)]. This phase is in reasonably good agreement with the design value.

Figure 4(a) shows the electric field intensity $|E_y|^2$ in an xy cross section through the center of the lens. The field distribution around each individual pillar element in the array is quite similar to the symmetric eigenmode calculated above for a pillar of the same size, confirming the unit cell approximation we made. Figures 4(b) and 4(c) show the real part of the E_y field component for yz and xz cross sections near the center of the structure and allow us to observe the curvature introduced by the structure. An xy cross section of the clearly defined focal spot is shown in Fig. 4(d). Figures 4(e) and 4(f) confirm that the focusing behavior is very similar for yz and xz cross sections. The actual focal length turns out to be somewhat larger than the analytical value, because the phase delay introduced is somewhat smaller than for the analytical case. This small deviation can be attributed to the assumption of a single pass phase delay and a symmetric eigenmode.

The focal spot has a near-circular shape [Fig. 4(d)]. It can be seen, however, that the intensity distribution in the focal spot does not exhibit exact 90° rotation symmetry. This is expected: for linearly polarized incident light, with the use of a lens with a large numerical aperture, there is in fact no reason a priori that the focal spot has to be circular [18]. The structure, however, is inherently polarization independent: the two polarizations behave in exactly the same way by rotational symmetry.

The flux directly underneath the lens divided by the incident flux of a reference measurement is 77%. As a point of comparison, a wavelength-size solid-state image sensor pixel with a dielectric shaped

Fig. 2.   (Color online) Basic building block for two-dimensional phase front design. (a) Real and imaginary parts of the effective index as a function of the base width s of the metal pillar. The inset shows the metal pillar, centered in the 100 nm by 100 nm unit cell. (b) Vector plot of the electric field in a unit cell with $s = 65$ nm.
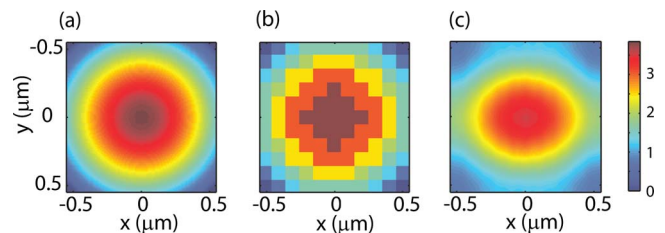
Fig. 3.   (Color online) Phase front design for wavelength-size metallic microlens. (a) Phase delay calculated analytically from Eq. (1). (b) Phase delay approximated by an array of unit cells. (c) Phase delay measured underneath the lens in a three-dimensional FDFD simulation.
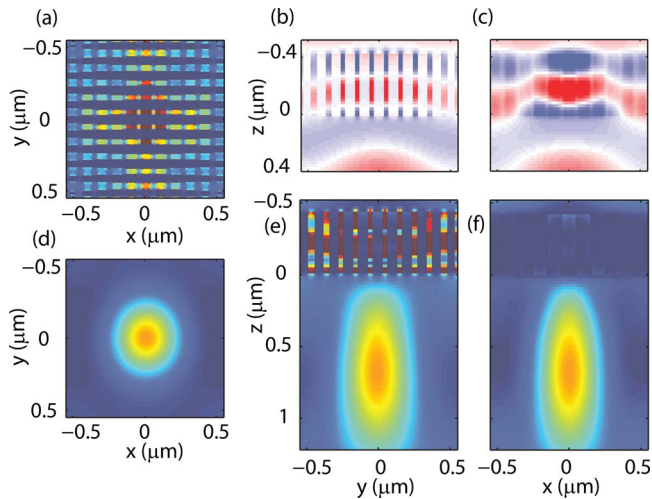
Fig. 4. (Color online) Two-dimensional focusing in a microlens application. (a) Electric field intensity $|E_y|^2$ for an xy cross section through the center of the lens structure (from Fig. 1). Real part of the E_y field for an (b) xy and (c) xz cross section near the center of the lens structure. (d)–(f) Electric field intensity $|E_y|^2$ for (d) xy, (e) yz, and (f) xz cross sections of the focal spot. Where necessary, the field intensities inside the gaps are saturated.

microlens has an optical efficiency of 67% [19], showing that the losses of the metallic microlens design are quite reasonable. Reflection of the structure is calculated at 9% and can likely be improved by optimization. Propagation losses inside the metallic structure are estimated at about 14%. Since the structure consists of 37% metal, funneling of light occurs in the gaps and transmission is slightly extraordinary. The intensity is locally modulated as well. This can be expected from a structure that is on resonance at certain locations, and off resonance in other places, but it is not detrimental to the structure's behavior.

Fabricating these structures using top-down approaches, including lithography or focused ion beam milling, might prove challenging owing to the high aspect ratios that are required. Fabrication requirements could be eased by increasing structure size and focal length. A bottom-up approach by growing the pillars could provide an alternative implementation method. In fact, the nanoscale pillar dimensions correspond well with realistic nanowire diameters [20,21]. In such a setup, local phase delay could be tuned by either pillar size or pillar density.

In conclusion, the presented design principles allow a nanophotonic component designer to tailor phase delay in wavelength-size devices by varying local geometry. Whereas we focused on a lens structure, the principles should be extendible to more complex designs, for instance to compensate for angles of incidence [9], or to intentionally introduce polarization dependence by using rectangular base instead of square base pillars. Similar structures, extended in the z direction, should also enable deep-subwavelength focusing within the structure, as we demonstrated before in a slit array [22].

References and Notes

1. N. Engheta, Science **317**, 1698 (2007).
2. V. M. Shalaev, Nat. Photonics **1**, 41 (2007).
3. S. Lal, S. Link, and N. J. Halas, Nat. Photonics **1**, 641 (2007).
4. Z. Sun and H. K. Kim, Appl. Phys. Lett. **85**, 642 (2004).
5. H. Shi, C. Wang, C. Du, X. Luo, X. Dong, and H. Gao, Opt. Express **13**, 6815 (2005).
6. T. Xu, C. Wang, C. Du, and X. Luo, Opt. Express **16**, 4753 (2008).
7. C. Min, P. Wang, X. Jiao, Y. Deng, and H. Ming, Opt. Express **15**, 9541 (2007).
8. L. Verslegers, P. B. Catrysse, Z. Yu, J. S. White, E. Barnard, M. L. Brongersma, and S. Fan, Nano Lett. **9**, 235 (2009).
9. L. Verslegers, P. B. Catrysse, Z. Yu, and S. Fan, Appl. Phys. Lett. **95**, 071112 (2009).
10. Z. Sun, Appl. Phys. Lett. **89**, 261119 (2006).
11. S. Yin, C. Zhou, X. Luo, and C. Du, Opt. Express **16**, 2578 (2008).
12. Y. Fu, W. Zhou, L. E. N. Lim, C. L. Du, and X. G. Luo, Appl. Phys. Lett. **91**, 061124 (2007).
13. D. R. Lide, ed., *CRC Handbook of Chemistry and Physics*, 88th ed. (CRC, 2007).
14. P. Ruffieux, T. Scharf, H. P. Herzig, R. Völkel, and K. J. Weible, Opt. Express **14**, 4687 (2006).
15. G. Veronis and S. Fan, Opt. Lett. **30**, 3359 (2005).
16. G. Veronis and S. Fan, in *Surface Plasmon Nanophotonics*, M. L. Brongersma and P. G. Kik, eds. (Springer, 2007), p. 169.
17. A detailed description of the three-dimensional FDFD method will be published elsewhere.
18. B. Richards and E. Wolf, Proc. R. Soc. London Ser. A **253**, 358 (1959).
19. C. C. Fesenmaier, Y. Huo, and P. B. Catrysse, Opt. Express **16**, 20457 (2008).
20. R. Yan, D. Gargas, and P. Yang, Nat. Photonics **3**, 569 (2009).
21. A. V. Kabashin, P. Evans, S. Pastkovsky, W. Hendren, G. A. Wurtz, R. Atkinson, R. Pollard, V. A. Podolskiy, and A. V. Zayats, Nat. Mater. **8**, 867 (2009).
22. L. Verslegers, P. B. Catrysse, Z. Yu, and S. Fan, Phys. Rev. Lett. **103**, 033902 (2009).